

Bahnhofsallee 1e  
37081 Göttingen  
Germany

5<sup>th</sup> December 2016

Dear Gerhard Herndl

**BG – 2016 - 251 Cavan et al.**

Please find enclosed a revised manuscript, figures and supplementary material and this point-by-point response to the reviews and a marked manuscript. Changes have been highlighted in this marked manuscript. We have addressed all the concerns of the reviewers of which the main was the requirement for more information on the conversion factors used and a sensitivity analysis.

We compared our particulate organic carbon (POC) mass using Alldredge (1998) conversion factors (CFs) to mass calculated using faecal pellet CFs by Manno et al. (2015) in the Southern Ocean (see supplementary material, Fig S2). There are no relevant CFs for phytodetrital aggregates in the literature. Both CFs produced similar results using the winter values from Manno et al. but the summer CFs overestimated POC compared to Alldredge. We also calculated particle export efficiency (PE<sub>eff</sub>) to see how using the different CFs would effect our results and conclusions; both CFs showed the same trend, decreasing PE<sub>eff</sub> with increasing primary production (Fig. S2). Hence using a different CF does not change the trends we observed or our conclusions. We have included text (lines 147-175) in the methods section to explain the choice of CFs and the sensitivity analysis with Manno et al.

The other main point from the reviewers was to include more information on the type of particle or dominate plankton groups. Whilst we did not have data from all three regions on the latter we have now shown the proportion of faecal pellets and phytodetrital aggregates to flux (Fig. S1). The SO was heavily dominated by FPs compared to the other two regions. We also added images of the different particles from each area (Fig. 2, lines 238-245).

Finally we included further discussion on how different dominant plankton groups might effect the efficiency of the biological carbon pump in different areas (lines 350 – 370). This draws on the conclusions from the Henson et al. (2012) study that shows latitudinal trends in transfer efficiency, potentially influenced by phytoplankton size and group.

We believe we have greatly enhanced the manuscript by including the conversion factor sensitivity analysis, which shows using a different CF does not alter our conclusions.

Many thanks for taking the time to review this resubmission.

Yours Sincerely,

Dr. Emma Cavan

1 **Role of zooplankton in determining the efficiency of the biological**  
2 **carbon pump**

3

4 Cavan, Emma. L. <sup>1\*</sup>, Henson, Stephanie. A. <sup>2</sup>, Belcher, Anna. <sup>1</sup> & Sanders,  
5 Richard. <sup>2</sup>

6

7 <sup>1</sup>University of Southampton, National Oceanography Centre, European Way,  
8 Southampton, SO14 3ZH, UK

9 <sup>2</sup>National Oceanography Centre, European Way, Southampton, SO14 3ZH, UK.

10

11 \*Corresponding author: Emma L. Cavan, University of Southampton, National  
12 Oceanography Centre, European Way, Southampton, SO14 3ZH, UK. (+44)  
13 2380 598724. [e.cavan@noc.soton.ac.uk](mailto:e.cavan@noc.soton.ac.uk).

14

15

16

17

18

19

20

21

22

23 **Abstract**

24 The efficiency of the ocean's biological carbon pump ( $BCP_{eff}$  – here the product of particle  
25 export and transfer efficiencies) plays a key role in the air-sea partitioning of  $CO_2$ . Despite  
26 its importance in the global carbon cycle, the biological processes that control  $BCP_{eff}$  are  
27 poorly known. We investigate the potential role that zooplankton play in the biological  
28 carbon pump using both *in situ* observations and model output. Observed and modelled  
29 estimates of fast, slow and total sinking fluxes are presented from three oceanic sites: the  
30 Atlantic sector of the Southern Ocean, the temperate North Atlantic and the equatorial Pacific  
31 oxygen minimum zone (OMZ). We find that observed particle export efficiency is inversely  
32 related to primary production likely due to zooplankton grazing, in direct contrast to the  
33 model estimates. The model and observations show strongest agreement in remineralization  
34 coefficients and  $BCP_{eff}$  at the OMZ site where zooplankton processing of particles in the  
35 mesopelagic zone is thought to be low. As the model has limited representation of  
36 zooplankton-mediated remineralization processes, we suggest that these results point to the  
37 importance of zooplankton in setting  $BCP_{eff}$ , including particle grazing and fragmentation,  
38 and the effect of diel vertical migration. We suggest that improving parameterizations of  
39 zooplankton processes may increase the fidelity of biogeochemical model estimates of the  
40 biological carbon pump. Future changes in climate such as the expansion of OMZs may  
41 decrease the role of zooplankton in the biological carbon pump globally, hence increasing its  
42 efficiency.

43

44 **Keywords**

45 Biological carbon pump, zooplankton, remineralization

46

47

## 48 1. Introduction

49

50 The biological carbon pump plays an important role in regulating atmospheric carbon dioxide  
51 levels (Kwon et al., 2009; Parekh et al., 2006). Phytoplankton in the surface ocean convert  
52 inorganic carbon during photosynthesis to particulate organic carbon (POC), a fraction of  
53 which is then exported out of the upper ocean. As particles sink through the interior ocean  
54 they are subject to remineralization by heterotrophs, such that only a small proportion of  
55 surface produced POC reaches the deep ocean (Martin et al. 1987). The efficiency of the  
56 biological carbon pump ( $BCP_{eff}$ , defined here as the proportion of surface primary  
57 production that is transferred to the deep ocean (Buesseler and Boyd, 2009) therefore affects  
58 the air-sea partitioning of  $CO_2$  (Kwon et al., 2009). Greater understanding on the controls of  
59 this term may consequently result in more accurate assessments of the BCP's role in the  
60 global carbon cycle.

61

62 One approach to determine  $BCP_{eff}$  over long time scales (millennia) is by assessing the  
63 relative proportions of preformed and regenerated nutrients, i.e. the fraction of upwelled  
64 nutrients that is removed from surface waters by biological uptake (Hilting et al., 2008).  
65 However to assess  $BCP_{eff}$  over much shorter timescales (days to weeks) we use the  
66 definition of Buesseler & Boyd (2009) where  $BCP_{eff}$  is the product of particle export  
67 efficiency ( $PE_{eff}$ , the ratio of exported flux to mixed layer primary production) and transfer  
68 efficiency ( $TE_{eff}$ , the ratio of deep flux to exported flux). Using these two parameters together  
69 allows a more in-depth analysis of the biological processes involved and thus the assessment  
70 of the role of zooplankton in setting  $BCP_{eff}$ . Additionally the attenuation coefficients  
71 Martin's  $b$  (Martin et al. 1987) and the remineralization length scale  $z^*$  (Boyd and Trull,

72 2007) are useful to quantify how rapidly exported POC is remineralized in the mesopelagic  
73 zone.  
74  
75  $PE_{eff}$  varies proportionally to primary production, although uncertainty exists as to whether  
76 the relationship is inverse or positive (Aksnes and Wassmann, 1993; Cavan et al., 2015;  
77 Henson et al., 2015; Laws et al., 2000; Maiti et al., 2013; Le Moigne et al., 2016). Potential  
78 controls on  $PE_{eff}$  include temperature (Henson et al., 2015; Laws et al., 2000), zooplankton  
79 grazing (Cavan et al., 2015), microbial cycling (Le Moigne et al., 2016), mineral ballasting  
80 (Armstrong et al., 2002; François et al., 2002; Le Moigne et al., 2012) or large export of  
81 dissolved organic carbon (Maiti et al., 2013).  $Te_{eff}$  and POC attenuation coefficients describe  
82 how much of the exported POC reaches the deep ocean and how much of it is remineralized.  
83 Essentially the attenuation of POC with depth is determined by the sinking rates of particles  
84 and how rapidly the POC is turned over (Boyd and Trull, 2007). However, these factors  
85 themselves are controlled by various other processes such as: ballasting by minerals  
86 (François et al., 2002; Le Moigne et al., 2012), epipelagic community structure (Lam et al.,  
87 2011), temperature (Marsay et al., 2015), lability of the particles (Keil et al., 2016) and  
88 zooplankton diel vertical migration (Cavan et al., 2015). Therefore it is unlikely that any  
89 single factor controls  $BCP_{eff}$ .

90  
91 The role of zooplankton in controlling the efficiency of the BCP is often overlooked, with  
92 greater focus on factors such as biominerals for ballasting (De La Rocha and Passow, 2007)  
93 or microbial respiration (Herndl and Reinthaler, 2013). Nevertheless zooplankton have the  
94 potential to significantly impact the biological carbon pump as they can consume and  
95 completely transform particles (Lampitt et al., 1990). Grazing by zooplankton results in POC  
96 either passing through the gut and being egested as a fecal pellet, being respired as  $CO_2$  or

97 fragmented into smaller particles through sloppy feeding (Lampitt et al., 1990). Further,  
98 zooplankton can undergo diel vertical migration, feeding on particles at night in the surface  
99 and egesting them at depth during the day (Wilson et al., 2013). Consequently a significant  
100 proportion of POC may escape remineralization in the upper mesopelagic zone (Cavan et al.,  
101 2015), where recycling of POC is most intense (Martin et al. 1987).

102

103 In this study we combine observations (made using Marine Snow Catchers, MSCs) and  
104 model output to investigate the role of zooplankton in setting the efficiency of the biological  
105 carbon pump in three different oceanic regions: the Atlantic sector of the Southern Ocean  
106 (SO), the Porcupine Abyssal Plain (PAP) site in the temperate North Atlantic and the  
107 Equatorial Tropical North Pacific (ETNP) oxygen minimum zone. The ecosystem model  
108 used here, MEDUSA (Yool et al., 2013), was chosen as it separates particle fluxes into slow  
109 and fast sinking groups. Additionally the only interactions of zooplankton with particles in  
110 MEDUSA are through the production of particles (fecal pellets) and by grazing on slow  
111 sinking particles only. Here we compare various indices of  $BCP_{eff}$  between the observations  
112 and model to infer the role of zooplankton in controlling  $BCP_{eff}$ .

113

## 114 **2. Methods**

### 115 **2.1 Site description**

116 Three very different sites were chosen in this study: the Atlantic sector of the Southern Ocean  
117 Ocean (SO, 45 – 65 °S, 20 – 70 °W), the Porcupine Abyssal Plain (PAP) site in the temperate  
118 North Atlantic (49 °N, 17 °W) and the Equatorial Tropical North Pacific (ETNP) oxygen  
119 minimum zone (13 °N, 91 °W) (Fig. 1). The SO accounts for ~ 20 % of the global ocean CO<sub>2</sub>  
120 uptake (Park et al., 2010; Takahashi et al., 2002) and is a large high-nutrient-low-chlorophyll  
121 region, in part due to limited iron availability (Martin, 1990). Nevertheless, iron from oceanic

122 islands and melting sea ice can cause intense phytoplankton blooms, which may lead to high  
123 POC export (Pollard et al., 2009). In the temperate North Atlantic seasonality is high, with  
124 phytoplankton blooms occurring in spring and summer (Lampitt et al., 2001). The region  
125 contributes disproportionally to global export, accounting for 5 – 18 % of the annual global  
126 export (Sanders et al., 2014). In the ETNP region a strong oxygen minimum (OMZ) persists  
127 where, between 50 and 1000 m depth, dissolved oxygen concentration can fall below 2  $\mu\text{mol}$   
128  $\text{kg}^{-1}$  (Paulmier and Ruiz-Pino, 2009). In OMZs the low oxygen concentrations may lead to a  
129 high transfer efficiency of POC flux potentially due to reduced heterotrophy (Devol and  
130 Hartnett, 2001; Hartnett et al., 1998; Keil et al., 2016; Van Mooy et al., 2002).

131

## 132 **2.2 Observations**

133 Particles were collected using Marine Snow Catchers (MSCs) (Riley et al., 2012) from the  
134 three oceanic sites as shown in Fig. 1. In total 27 stations were sampled, 18 in the SO, 5 at  
135 PAP and 4 in the ETNP (Table S1). MSCs have the advantage of being able to separate  
136 particles intact into two groups dependent on their sinking rate, fast ( $> 20 \text{ m d}^{-1}$ ) or slow ( $<$   
137  $20 \text{ m d}^{-1}$ ). MSCs were deployed below the mixed layer depth (MLD), which was determined  
138 as the depth with the steepest gradient of salinity and temperature, and usually occurred  
139 between 20 and 70 m (Table S1). The shallowest MSC was deployed 10 m below the MLD  
140 and another 100 m deeper than this for the Southern Ocean (Cavan et al., 2015) and the PAP  
141 site. In the ETNP MSCs were also deployed deeper into the water column to a maximum  
142 depth of 220 m.

143

144 Fast and slow sinking particles were collected from the MSC following the protocol by Riley  
145 et al. (Riley et al., 2012). Images of fast sinking particles were taken to estimate the  
146 equivalent spherical diameter (ESD) of the particles and ESD converted to POC mass *via*

147 conversion factors, CFs (Alldredge, 1998; Cavan et al., 2015). Two different CFs were used,  
148 one for phytodetrital aggregates (PDAs, Eq 1) and one for faecal pellets (FPs, Eq 2):

149 
$$\text{Phytodetrital aggregates} \quad m = 1.09 * V^{0.52} \quad (\text{Equation 1})$$

150 
$$\text{Faecal pellets} \quad m = 1.05 * V^{0.51} \quad (\text{Equation 2})$$

151 where  $m$  is mass of POC and  $V$  volume of the particle. Very few published studies exist  
152 comparing size of particles to carbon content, and those that do tend to focus on FPs (Manno  
153 et al., 2015). We chose to use the Alldredge (1998) CF because it allows comparison with  
154 other published studies (e.g. Ebersbach and Trull, 2008; Guidi et al., 2007; Laurenceau et al.,  
155 2015; Riley et al., 2012, Belcher et al., 2016), describes the fractal nature of particles and is  
156 an upper ocean study (50 % of our observations lie close to the depth (~20 m) of the  
157 Alldredge (1998) particles; Table S1). Another important point is that the MSCs allow  
158 collection of particles relatively undamaged or unaltered compared to sediment traps (other  
159 than gel traps), making the use of conversion factors more reliable as particle shapes reflect  
160 those measured *in situ* (Romero-Ibarra and Silverberg, 2011).

161  
162 To test the robustness of the Alldredge (1998) CFs we compared the resulting POC mass with  
163 that calculated using the CFs from Manno et al. (2015). This study was done in the Southern  
164 Ocean and only focussed on FPs, hence we only tested the similarity using our SO data where  
165 FPs comprised most (> 60 %) of the particle flux (Fig. S1). Manno et al. found a linear  
166 relationship between FP size and POC content for cylindrical FPs ( $0.018 \text{ mg C mm}^{-3}$ ). We  
167 calculated the total fast sinking POC mass (FP + PDA) using the Manno CF for FPs and  
168 Alldredge CFs for the PDAs (remembering that FPs dominated flux) and compared these to  
169 just using the Alldredge CFs (Fig. S2 a). The slope of the regression between the two is very  
170 close to 1 at 0.96 showing neither CF under- or over estimates POC relative to the other.  
171 There was no statistical difference (t-test,  $t = 0.25$ ,  $df = 77.23$ ,  $p\text{-value} = 0.80$ ) between the



172 mean masses of the two methods, with Manno CFs producing a mean mass of POC per  
173 sample of 11  $\mu\text{g C}$  and Alldredge CFs producing a mean of 8.4  $\mu\text{g C}$ . Therefore we conclude  
174 that using the Alldredge CFs is justified and using one general CF allows comparisons  
175 between our different study regions.

176

177 Slow sinking and suspended particles were filtered onto ashed (400 °C, overnight) GF/F  
178 filters and run in a HNC elemental analyser to determine POC mass. Sinking rates were  
179 estimated for fast sinking particles in the SO and at PAP by placing particles into a measuring  
180 cylinder filled with *in situ* sea water and timing how long it took each particle to pass a  
181 discrete point (Cavan et al., 2015). At the ETNP a FlowCAM was used to measure fast  
182 particle sinking rates (Bach et al., 2012). All slow sinking particle rates were calculated using  
183 the SETCOL method (Bienfang, 1981). Fluxes ( $\text{mg C m}^{-2} \text{d}^{-1}$ ) were calculated by dividing the  
184 mass of POC (mg) by the area of the MSCs ( $\text{m}^2$ ) and the sinking time of the particles (d)  
185 (Cavan et al., 2015). Primary production (PP) was estimated from 8-day satellite-derived data  
186 using the Vertically Generalised Productivity Model (Behrenfeld and Falkowski, 1997)  
187 applied to MODIS data.

188

### 189 **2.3 Model output**

190 The ecosystem model MEDUSA (Yool et al., 2013) was used for this study as it distinguishes  
191 detrital fluxes in two pools, fast and slow sinking. In MEDUSA, fast sinking particles are  
192 assumed to sink more rapidly than the time-step of the model and are remineralized  
193 instantaneously at all vertical levels with the flux profile determined by a ballast model  
194 (Armstrong et al., 2002). Slow sinking particles sink at  $3 \text{ m d}^{-1}$  and remineralization is  
195 temperature dependent, with zooplankton grazing on slow sinking particles but not on the fast  
196 sinking particles. Zooplankton DVM is not parameterised. Primary production is modelled as

197 non-diatom and diatom production, which is summed to give the total depth-integrated  
198 primary production. The model was run in hindcast mode at  $\frac{1}{4}^\circ$  spatial resolution and output  
199 saved with a 5-day temporal resolution. The model output was extracted at the same locations  
200 and times as the observations were made and averaged over 12 years (1994 - 2006) to give  
201 the climatological seasonal cycle. The model outputs fluxes of particulate organic nitrogen  
202 ( $\text{mg N m}^{-2} \text{d}^{-1}$ ) which are converted to POC ( $\text{mg C m}^{-2} \text{d}^{-1}$ ) using the Redfield ratio (Redfield,  
203 1934).

204

## 205 **2.4 Data manipulation**

206 For both the observations and the model output the fast and slow sinking fluxes were  
207 summed to calculate the total sinking POC flux. Model output was available at fixed depths  
208 of 100 and 200 m, which introduces an offset with our at-sea observations (Table S1). This  
209 study is therefore assessing  $BCP_{eff}$  in the upper ocean only. Parameters calculated to test the  
210 efficiency of the biological carbon pump were the percentage contribution of fast and slow  
211 sinking particles to the total sinking flux, particle export efficiency ( $PE_{eff}$ ), the attenuation of  
212 flux with depth expressed as  $b$  and  $z^*$  and transfer efficiency ( $Te_{eff}$ ).

213

214  $PE_{eff}$  is the proportion of surface produced primary production (PP) that is exported out of  
215 the mixed layer (observations) or at 100 m (model) and is calculated by dividing the exported  
216 flux by PP. To estimate the attenuation of flux over the upper mesopelagic zone the  
217 exponents  $b$  (Martin et al. 1987) and  $z^*$  (Buesseler and Boyd, 2009) were calculated, where  
218 fluxes at the export depth and 100 m below were used for observations and fluxes at 100 and  
219 200 m from the model. The  $b$  exponent is dimensionless and generally ranges from 0 to 1.5  
220 with low values indicating low attenuation, thus low remineralization, and higher values  
221 representing high attenuation and remineralization. The  $z^*$  (m) exponent is the

222 remineralization length scale, or the depth by which only 37 % of the reference flux (here at  
223 the export depth) remains. Thus a large  $z^*$  suggests low attenuation and low remineralization  
224 of the particle flux. The  $T_{eff}$  is another parameter that represents how much flux reaches the  
225 deeper ocean and hence is not remineralized. This is simply calculated by dividing the deep  
226 flux (125 – 220 m in observations and 200 m in model) by the export flux. All indices are  
227 dimensionless apart from  $z^*$  which is in metres.

228

### 229 **3. Results and Discussion**

#### 230 **3.1 Comparison of fluxes**

231 We compare model output with satellite-derived estimates of primary production (PP), POC  
232 export and deep (150 - 300 m) fluxes in the upper ocean (Fig. S3). Overall, modelled PP  
233 compares well compared to satellite-derived estimates with a strong positive correlation  
234 between the two ( $p < 0.001$ ,  $r^2 = 0.84$ , Fig. S3 a), although the model slightly overestimates  
235 PP. When comparing the total sinking export fluxes and total deep fluxes, most points lie  
236 below the 1:1 line, suggesting that the model is overestimating POC flux (Figs. S3 b & c).

237

#### 238 **3.2 Observed particles**

239 In all three regions particles were classified as phytodetrital aggregates (PDAs) or faecal  
240 pellets (FPs) using the images taken. PDAs were of a similar aesthetic nature in all three  
241 areas (Fig. 2) consisting of unidentifiable (to phytoplankton species level) detrital material. In  
242 the SO FPs were either from krill which form long chains of pellets (Fig. 2b) or copepods  
243 (Wilson et al., 2008). At PAP and in the ETNP, only copepod FPs were observed (Fig. 2 d &  
244 f). FPs dominated particle flux in the SO but PDAs dominated at PAP and in the ETNP (Fig.  
245 S1)

246

### 247 3.3 Export production

248 The traditional view of export production is that as PP increases, so does POC export out of  
249 the mixed layer (Laws et al., 2000). However recent analyses from the Southern Ocean (SO)  
250 observe the opposite relationship, that an inverse relationship between  $PE_{eff}$  and PP exists  
251 (Cavan et al., 2015; Maiti et al., 2013; Le Moigne et al., 2016). We find that for fast sinking  
252 particles the model shows  $PE_{eff}$  increases with PP (Fig. 3 a) according to a power law  
253 function ( $p < 0.001$ ,  $r^2 = 0.6$ ) while the observations show an inverse relationship (logarithmic  
254 function,  $p < 0.001$ ,  $r^2 = 0.4$ ), even when including sites outside of the SO. This inverse  
255 relationship was preserved for the SO when including conversion factors of Manno et al.  
256 (2015) (Fig. S2b).

257

258 However for the slow sinking particles the model shows an inverse relationship between PP  
259 and  $PE_{eff}$ , similar to that seen in the observations for the fast sinking particles (power law  
260 function,  $p < 0.001$ ,  $r^2 = 0.97$ , Fig. 3 b). Potential reasons for an inverse relationship between PP  
261 and  $PE_{eff}$  include the temporal decoupling between primary production and export (Salter et  
262 al., 2007), seasonal dynamics of the zooplankton community (Tarling et al., 2004) or grazing  
263 by zooplankton (Cavan et al., 2015; Maiti et al., 2013; Le Moigne et al., 2016). As previously  
264 mentioned one of the differences between the fast and slow sinking detrital pools in the  
265 model is that slow sinking particles are grazed on by zooplankton and fast sinking are not.  
266 Thus when zooplankton graze on particles in the model an inverse relationship between  $PE_{eff}$   
267 and PP exists and when zooplankton grazing is not accounted for, the opposite occurs. This  
268 highlights the importance of zooplankton in determining the efficiency of the BCP.

269

270 The observed slow sinking  $PE_{eff}$  were generally very low ( $< 0.05$ ) and thus had little  
271 influence on the  $PE_{eff}$  for total sinking POC flux, which also had a non-linear inverse

272 relationship with PP ( $p < 0.001$ ,  $r^2 = 0.4$ , Fig. 3 c). It is important to note that high values of  
273 PP ( $> 1000 \text{ mg C m}^{-2} \text{ d}^{-1}$ ) were only present at PAP, and that the SO had the greatest range of  
274 PP, so drives a large part of the inverse relationship. Therefore measuring  $PE_{eff}$  in other  
275 regions with large PP ranges is fundamental to see if this relationship holds outside the sites  
276 from this study.

277

### 278 **3.4 Contribution of fast and slow sinking POC fluxes**

279 Particles naturally sink at different rates, with one operational definition being that slow  
280 sinking particles sink at  $< 20 \text{ m d}^{-1}$  and fast sinking particles at  $> 20 \text{ m d}^{-1}$  (Riley et al., 2012).  
281 Most sediment traps cannot separately measure fluxes of fast and slow sinking particles and  
282 are unlikely to capture much of the slow sinking flux due to their deployment in the lower  
283 mesopelagic and bathypelagic zones (Buesseler et al., 2007; Lampitt et al., 2008). Slow  
284 sinking particles may sink too slowly and be remineralized too quickly to reach the deep  
285 ocean unless they are formed there. Hence the MSC is a useful tool to analyse the two  
286 sinking fluxes separately.

287

288 In both the model and the observations, the slow sinking flux was consistently smaller than  
289 the fast sinking flux and generally only contributed  $< 40 \%$  of the total flux (Fig. S4).  
290 However in the model the proportion of slow sinking flux always decreases with depth (Figs.  
291 S4 a-c) whereas observations at the PAP site showed the proportion of slow sinking fluxes  
292 increased with depth (Figs. S4 e). Increases in slow sinking particles with depth must be from  
293 the fragmentation of larger fast sinking particles either abiotically (Alldredge et al., 1990) or  
294 from sloppy feeding by zooplankton (Lampitt et al., 1990) or advection or mixing  
295 (Dall'Olmo et al., 2016). Sloppy feeding results in zooplankton fragmenting particles into  
296 smaller particles resulting in a larger surface area to volume ratio increasing colonization by

297 microbes and thus remineralization (Mayor et al., 2014). Zooplankton do not graze on fast  
298 sinking particles in the model hence neither sloppy feeding nor abiotic fragmentation are  
299 represented (Yool et al., 2013). This likely explains why the contribution of slow sinking  
300 particles can only decrease with depth in the model, unlike the observations in which slow  
301 sinking particles may increase with depth.

302

### 303 **3.5 Attenuation of POC with depth**

304 The attenuation of POC through the water column describes how quickly POC fluxes are  
305 remineralized, with a high attenuation indicating high POC remineralization. We used the  
306 parameters  $b$  (Martin et al. 1987) and  $z^*$  (Boyd and Trull, 2007) to describe the attenuation of  
307 flux with depth. A recent study suggests POC remineralization is temperature dependent  
308 (Marsay et al., 2015) hence we compared the attenuation coefficients with temperature.

309 Calculated mean  $b$  and  $z^*$  values for total (fast + slow) sinking POC from the model were  
310 similar at all sites (Figs. 4 a & b) with no correspondence with temperature, even though slow  
311 sinking particles are remineralized as a function of temperature in the model. Hence slow  
312 sinking  $b$  and  $z^*$  increase and decrease respectively with temperature (Table S2). The  
313 observations (for total sinking particles) show a non-linear relationship with temperature that  
314 deviates away from the Marsay et al. (2015) regression, such that remineralization increases  
315 (high attenuation) at temperatures greater than 13 °C. The variability is much greater in the  
316 observations than the model, a feature that is consistent across all indices (Figs. 4 a & b).

317 Apart from at the ETNP where the model and observations agree, the observations  
318 consistently show slower POC attenuation compared to the model. The active transfer of  
319 POC to depth *via* diel vertical migration (DVM) of zooplankton (Wilson et al., 2008) may  
320 contribute to the observed slower rates of POC attenuation. Cavan et al. 2015 showed that  
321 high Southern Ocean  $b$  values were a result of DVM, a process not parameterized in the

322 MEDUSA model. Although active transfer *via* DVM is a complex process that may be  
323 difficult to model, it is potentially important to include in biogeochemical models, as it has  
324 been shown to account for 27 % of the total flux in the North Atlantic (Hansen and Visser,  
325 2016).

326

327 The strong alignment of the modelled and observed attenuation at the ETNP is likely because  
328 of the lack of particle processing by zooplankton, by design in the model and naturally in  
329 oxygen minimum zones (OMZs). The daytime depth of vertically migrating zooplankton is  
330 reduced in OMZs due to low dissolved oxygen concentrations (Bianchi et al., 2013), which at  
331 the ETNP reach  $< 2 \mu\text{mol kg}^{-1}$  by 120 m. Further the population of zooplankton below this  
332 depth is almost non-existent in OMZs (Wishner et al., 2013) and those that are there feed on  
333 particles at the surface, not in the OMZ core (Williams et al., 2014). Thus zooplankton  
334 consumption and manipulation of particles is greatly reduced in OMZs and is non-existent in  
335 the MEDUSA model.

336

### 337 **3.6 Efficiency of the biological carbon pump**

338 To calculate  $BCP_{eff}$  (proportion of mixed layer primary production found at depth, here 150 -  
339 300 m) we replicated the  $BCP_{eff}$  plots of Buesseler & Boyd (2009) by plotting  $PE_{eff}$  against  
340 transfer efficiency ( $T_{eff}$ ) for fast, slow and total sinking particles (Fig. 5). According to the  
341 observations, the SO had the highest total sinking  $BCP_{eff}$  at 40 %, similar to the maximum  
342 observed by Buesseler & Boyd (2009) in the North Atlantic. The SO observations showed a  
343 higher  $BCP_{eff}$  than the model by about 10 % across all sinking fluxes (Fig. 5). This  
344 difference was largely due to a very high  $T_{eff}$  ( $> 1$ ) estimated from observations, which  
345 implies fluxes increased at depth. This could be due to active fluxes by vertically migrating  
346 zooplankton, possibly krill (Cavan et al., 2015). Active fluxes could account for high

347 observed  $T_{eff}$  in the slow sinking particles, as well as fragmentation of larger particles at  
348 depth (Mayor et al., 2014).

349

350  $T_{eff}$  is often thought to be controlled by the dominant phytoplankton group in the upper  
351 ocean, which is linked to the ballasting hypothesis (Francois et al., 2002; Henson et al.,  
352 2012).  $T_{eff}$  for total POC flux estimated by the model (Fig. 5 c) is roughly the same in all  
353 three regions, even though the MEDUSA model is capable of altering the ratio of diatom to  
354 non-diatom PP (Yool et al., 2013), as would be expected when comparing the Southern  
355 Ocean and the Equatorial Pacific. Diatoms often dominate the SO (Salter et al., 2007) whilst  
356 the ETNP is dominated by pico- and nanophytoplankton (Puigcorb  et al., 2015), and at the  
357 PAP site a range of phytoplankton species are found from diatoms to smaller cyanobacteria  
358 and dinoflagellates (Smythe-Wright et al., 2010).

359

360 In this study we observe the opposite trend in  $T_{eff}$  compared to Henson et al. (2012) with the  
361 SO exhibiting high  $T_{eff}$  ( $> 1$ ) and the ETNP the lowest ( $\sim 0.5$ ). This could be due to the depth  
362 range over which  $T_{eff}$  is calculated as here it is relatively shallow ( $< 200$  m) compared to the  
363 2000 m range in Henson et al. (2012). For instance, Henson et al. (2012) estimate  $T_{eff}$  of  $\sim$   
364 0.4 in the ETNP, very close to the calculated values in this study, which due to the  
365 hypothesised lack of zooplankton interactions with particles in the deep OMZs could remain  
366 unchanged if calculated at 2000 m depth. However, in the SO zooplankton influence particle  
367 transfer heavily and thus if we had observed  $T_{eff}$  at 2000 m, it may have been much lower,  
368 and conform to the finding that at high latitudes  $P_{E_{eff}}$  is high and  $T_{eff}$  is low (Henson et al.,  
369 2012). This highlights the potential complex interactions between particles and zooplankton  
370 in the upper mesopelagic zone which may be missed in deep ocean particle studies.

371



372 Even though the PAP site had the highest PP, the  $BCPe_{eff}$  was lowest ( $< 15\%$ ). There were  
373 also large differences (up to  $15\%$ ) in the  $BCPe_{eff}$  between the model and the observations at  
374 the PAP site driven by large discrepancies in  $PE_{eff}$ . Observations of fast sinking  $PE_{eff}$  were  
375 much lower than predicted by the model (Fig. 5 a), which we suggest could result from active  
376 grazing and fragmentation of fast sinking particles by zooplankton.  $Te_{eff}$  of fast sinking  
377 particles was low and consistent with model predictions, suggesting that active transfer via  
378 DVM (not parameterized in the model) plays a relatively minor role at the PAP site.  
379 Therefore mineral ballasting (Armstrong et al., 2002), which drives  $Te_{eff}$  in the model, may be  
380 the main driver of  $Te_{eff}$  at PAP. The modelled and observed slow sinking  $BCPe_{eff}$  were similar  
381 at PAP ( $\sim 1\%$ ) despite a large difference in  $Te_{eff}$  (Fig. 5 b). Fragmentation of fast to slow  
382 sinking particles (not included in the model) at depth could explain the difference in slow  
383 sinking  $Te_{eff}$ .

384

385 Finally the  $BCPe_{eff}$  for the ETNP is very similar between the model and observations for all  
386 sinking fluxes (Fig. 5). The similarity in the  $BCPe_{eff}$  here echoes the similarity shown for  
387 POC attenuation with depth. This reiterates our hypothesis that the model and observations  
388 agree on  $BCPe_{eff}$  only in areas of the global ocean where processing of particles by  
389 zooplankton is reduced due to very low dissolved oxygen concentrations.

390

#### 391 **4. Conclusions**

392 We have used observations and model output from the upper mesopelagic zone in 3  
393 contrasting oceanic regions to assess the influence of zooplankton on the efficiency of the  
394 biological carbon pump. We separately collected *in situ* fast and slow sinking particles, which  
395 are also separated into discrete classes in the MEDUSA model. The model has limited

396 processing of particles by zooplankton with only slow sinking detrital POC being grazed  
397 upon.

398

399 Our results highlight the crucial role that zooplankton play in regulating the efficiency of the  
400 biological carbon pump through 1) controlling particle export by grazing, 2) fragmenting  
401 large, fast sinking particles into smaller, slower sinking particles and 3) active transfer of  
402 POC to depth *via* diel vertical migration. Comparisons of the model and observations in an  
403 oxygen minimum zone provide strong evidence of the importance of zooplankton in  
404 regulating the BCP. Here extremely low dissolved oxygen concentrations at depth reduce the  
405 abundance and metabolism of zooplankton in the mid-water column. Thus the ability of  
406 zooplankton to degrade or repackage particles is vastly reduced in OMZs, and as such it is  
407 here that the model, with limited zooplankton interaction with particles, shows the strongest  
408 agreement with observations.

409

410 We recommend that grazing on large, fast sinking particles and the fragmentation of fast to  
411 slow sinking particles (either *via* zooplankton or abiotically) is introduced into global  
412 biogeochemical models, with the aim of also incorporating active transfer. Future changes in  
413 climate such as the expansion of OMZs may decrease the role of zooplankton in the  
414 biological carbon pump globally, increasing its efficiency and hence forming a positive  
415 climate feedback.

416

#### 417 **Acknowledgements**

418 We would like to thank all participants and crew on cruises JR274, JC087, JC097. Thanks to  
419 Annike Moje for running all POC samples in Bremen, Germany. Thanks also to Andrew  
420 Yool for providing the MEDUSA model output.

421 **References**

422

423 Aksnes, D. and Wassmann, P.: Modeling the significance of zooplankton grazing for export  
424 production, *Limnol. Oceanogr.*, 38(5), 978–985, 1993.

425 Alldredge, A.: The carbon, nitrogen and mass content of marine snow as a function of  
426 aggregate size, *Deep. Res. I*, 45(4-5), 529–541, 1998.

427 Alldredge, A., Granata, T. C., Gotschalk, C. C. and Dickey, T. D.: The physical strength of  
428 marine snow and its implications for particle disaggregation in the ocean, *Limnol. Oceanogr.*,  
429 35(November), 1415–1428, doi:10.4319/lo.1990.35.7.1415, 1990.

430 Armstrong, R., Lee, C., Hedges, J., Honjo, S. and Wakeham, S.: A new, mechanistic model  
431 for organic carbon fluxes in the ocean based on the quantitative association of POC with  
432 ballast minerals, *Deep. Res. II*, 49(1-3), 219–236, 2002.

433 Bach, L. T., Riebesell, U., Sett, S., Febiri, S., Rzepka, P. and Schulz, K. G.: An approach for  
434 particle sinking velocity measurements in the 3-400  $\mu\text{m}$  size range and considerations on the  
435 effect of temperature on sinking rates., *Mar. Biol.*, 159(8), 1853–1864, doi:10.1007/s00227-  
436 012-1945-2, 2012.

437 Behrenfeld, M. J. and Falkowski, P. G.: Photosynthetic rates derived from satellite-based  
438 chlorophyll concentration, *Limnol. Oceanogr.*, 42(1), 1–20, 1997.

439 Belcher, A., Iversen, M. H., Manno, C., Henson, S. A., Tarling, G. A. and Sanders, R.: The  
440 role of particle associated microbes in remineralisation of faecal pellets in the upper  
441 mesopelagic of the Scotia Sea, Antarctica, *Limnol. Oceanogr.*, 61, 1049–1064,  
442 doi:10.1002/lno.10269, 2016.

443 Bianchi, D., Stock, C., Galbraith, E. D. and Sarmiento, J. L.: Diel vertical migration :  
444 Ecological controls and impacts on the biological pump in a one-dimensional ocean model ,  
445 27(February), 1–14, doi:10.1002/gbc.20031, 2013.

446 Bienfang, P.: SETCOL - A technologically simple and reliable method for measuring  
447 phytoplankton sinking rates, *Can. J. Fish. Aquat. Sci.*, 38(10), 1289–1294, 1981.

448 Boyd, P. and Trull, T.: Understanding the export of biogenic particles in oceanic waters: Is  
449 there consensus?, *Prog. Oceanogr.*, 72(4), 276–312, doi:doi:10.1016/j.pocean.2006.10.007,  
450 2007.

451 Buesseler, K. and Boyd, P.: Shedding light on processes that control particle export and flux  
452 attenuation in the twilight zone of the open ocean, *Limnol. Oceanogr.*, 54(4), 1210–1232,  
453 2009.

454 Buesseler, K., Antia, A. N., Chen, M., Fowler, S. W., Gardner, W. D., Gustafsson, O.,  
455 Harada, K., Michaels, A. F., van der Loeff<sup>o</sup>, M. R., Sarin, M., Steinberg, D. K. and Trull, T.:  
456 An assessment of the use of sediment traps for estimating upper ocean particle fluxes, *J. Mar.*  
457 *Res.*, 65(3), 345–416, 2007.

458 Cavan, E. L., Le Moigne, F. A. C., Poulton, A. J., Tarling, G. A., Ward, P., Daniels, C. J.,  
459 Fragoso, G. M. and Sanders, R. J.: Attenuation of particulate organic carbon flux in the  
460 Scotia Sea, Southern Ocean, is controlled by zooplankton fecal pellets, *Geophys. Res. Lett.*,  
461 42(3), 821–830, 2015.

462 Dall’Olmo, G., Dingle, J., Polimene, L., Brewin, R. J. W. and Claustre, H.: Substantial  
463 energy input to the mesopelagic ecosystem from the seasonal mixed-layer pump, *Nat. Geosci.*,  
464 9(11), 820–823 [online] Available from: <http://dx.doi.org/10.1038/ngeo2818>, 2016.

465 Devol, A. H. and Hartnett, H. E.: Role of the oxygen-deficient zone in transfer of organic  
466 carbon to the deep ocean, *Limnol. Oceanogr.*, 46(7), 1684–1690,  
467 doi:10.4319/lo.2001.46.7.1684, 2001.

468 Ebersbach, F. and Trull, T. W.: Sinking particle properties from polyacrylamide gels during  
469 the Kerguelen Ocean and Plateau compared Study (KEOPS): Zooplankton control of carbon  
470 export in an area of persistent natural iron inputs in the Southern Ocean, *Limnol. Oceanogr.*,

471 53(1), 212–224, doi:10.4319/lo.2008.53.1.0212, 2008.

472 Francois, R., Honjo, S., Krishfield, R. and Manganini, S.: Factors controlling the flux of  
473 organic carbon to the bathypelagic zone of the ocean, *Global Biogeochem. Cycles*, 16(4), 34–  
474 1–34–20, doi:10.1029/2001GB001722, 2002.

475 François, R., Honjo, S., Krishfield, R. and Manganini, S.: Factors controlling the flux of  
476 organic carbon to the bathypelagic zone of the ocean, *Global Biogeochem. Cycles*, 16(4),  
477 1087, doi:doi:10.1029/2001GB001722, 2002, 2002.

478 Guidi, L., Stemmann, L., Legendre, L., Picheral, M., Prieur, L. and Gorsky, G.: Vertical  
479 distribution of aggregates (>110 µm) and mesoscale activity in the northeastern Atlantic:  
480 Effects on the deep vertical export of surface carbon, *Limnol. Oceanogr.*, 52(1), 7–18,  
481 doi:10.4319/lo.2007.52.1.0007, 2007.

482 Hansen, A. N. and Visser, A. W.: Carbon export by vertically migrating zooplankton: an  
483 adaptive behaviour model., *Prepr. Submitt. to Mar. Ecol. Prog. Ser.*, doi:10.1002/lno.10249,  
484 2016.

485 Hartnett, H. E., Devol, A. H., Keil, R. G., Hedges, J. and Devol, A. H.: Influence of oxygen  
486 exposure time on organic carbon preservation in continental margin sediments, *Nature*,  
487 391(February), 2–4, 1998.

488 Henson, S., Sanders, R. and Madsen, E.: Global patterns in efficiency of particulate organic  
489 carbon export and transfer to the deep ocean, *Global Biogeochem. Cycles*, 26(1028), 14,  
490 doi:doi:10.1029/2011GB004099, 2012.

491 Henson, S., Yool, A. and Sanders, R.: Variability in efficiency of particulate organic carbon  
492 export: A model study, *Global Biogeochem. Cycles*, 33–45,  
493 doi:10.1002/2014GB004965.Received, 2015.

494 Herndl, G. and Reinthaler, T.: Microbial control of the dark end of the biological pump., *Nat.*  
495 *Geosci.*, 6(9), 718–724, doi:10.1038/ngeo1921, 2013.

496 Hilting, A. K., Kump, L. R. and Bralower, T. J.: Variations in the oceanic vertical carbon  
497 isotope gradient and their implications for the Paleocene-Eocene biological pump,  
498 *Paleoceanography*, 23(3), PA3222, doi:10.1029/2007PA001458, 2008.

499 Keil, R. G., Neibauer, J., Biladeau, C., van der Elst, K. and Devol, A. H.: A multiproxy  
500 approach to understanding the “enhanced” flux of organic matter through the oxygen  
501 deficient waters of the Arabian Sea, *Biogeosciences*, 13, 2077–2092, doi:10.5194/bgd-12-  
502 17051-2015, 2016.

503 Kwon, E., Primeau, F. and Sarmiento, J.: The impact of remineralization depth on the air-sea  
504 carbon balance, *Nat. Geosci.*, 2, 630–635, 2009.

505 De La Rocha, C. and Passow, U.: Factors influencing the sinking of POC and the efficiency  
506 of the biological carbon pump, *Deep Sea Res. Part II Top. Stud. Oceanogr.*, 54(5-7), 639–  
507 658, doi:10.1016/j.dsr2.2007.01.004, 2007.

508 Lam, P. J., Doney, S. C. and Bishop, J. K. B.: The dynamic ocean biological pump: insights  
509 from a global compilation of Particulate Organic Carbon, CaCO<sub>3</sub> and opal concentrations  
510 profiles from the mesopelagic., *Global Biogeochem. Cycles*,  
511 doi:doi:10.1029/2010GB003868, 2011.

512 Lampitt, R., Noji, T. and Bodungen, B.: What happens to zooplankton faecal pellets?  
513 Implications for vertical flux, *Mar. Biol.*, 23, 15–23, 1990.

514 Lampitt, R., Bett, B., Kiriakoulakis, K., Popova, E., Ragueneau, O., Vangriesheim, A. and  
515 Wolff, G. A.: Material supply to the abyssal seafloor in the Northeast Atlantic, *Prog.*  
516 *Oceanogr.*, 50(1-4), 27–63, 2001.

517 Lampitt, R. S., Boorman, B., Brown, L., Lucas, M., Salter, I., Sanders, R., Saw, K., Seeyave,  
518 S., Thomalla, S. J. and Turnewitsch, R.: Particle export from the euphotic zone: Estimates  
519 using a novel drifting sediment trap, Th-234 and new production, *Deep. Res. Part I-*  
520 *Oceanographic Res. Pap.*, 55(11), 1484–1502, doi:DOI 10.1016/j.dsr.2008.07.002, 2008.

521 Laurenceau, E., Trull, T. W., Davies, D. M., Bray, S. G., Doran, J., Planchon, F. and Carlotti,  
522 F.: The relative importance of phytoplankton aggregates and zooplankton fecal pellets to  
523 carbon export : insights from free-drifting sediment trap deployments in naturally iron-  
524 fertilised waters near the Kerguelen Plateau, , 1007–1027, doi:10.5194/bg-12-1007-2015,  
525 2015.

526 Laws, E., Falkowski, P. G., Smith, W. O., Ducklow, H. and McCarthy, J. J.: Temperature  
527 effects on export production in the open ocean, *Global Biogeochem. Cycles*, 14(4), 1231–  
528 1246 [online] Available from: <Go to ISI>://000166341000019, 2000.

529 Maiti, K., Charette, M. a., Buesseler, K. O. and Kahru, M.: An inverse relationship between  
530 production and export efficiency in the Southern Ocean, *Geophys. Res. Lett.*, 40(November  
531 2012), doi:10.1002/grl.50219, 2013.

532 Manno, C., Stowasser, G., Enderlein, P., Fielding, S. and Tarling, G. A.: The contribution of  
533 zooplankton faecal pellets to deep-carbon transport in the Scotia Sea (Southern Ocean),  
534 *Biogeosciences*, 12(6), 1955–1965, doi:10.5194/bg-12-1955-2015, 2015.

535 Marsay, C., Sanders, R., Henson, S., Pabortsava, K., Achterberg, E. and Lampitt, R.:  
536 Attenuation of sinking particulate organic carbon flux through the mesopelagic ocean, *Proc.*  
537 *Natl. Acad. Sci.*, 12(4), 1089–1094, 2015.

538 Martin, J., Knauer, G., Karl, D. and Broenkow, W.: VERTEX: carbon cycling in the north  
539 east Pacific, *Deep. Res.*, 34(2), 267–285, 1987a.

540 Martin, J. H.: Glacial-interglacial CO<sub>2</sub> change: the iron hypothesis,  
541 *Paleoceanography|Paleoceanography*, 5(1), 1–13 [online] Available from: <Go to  
542 ISI>://INSPEC:3655190, 1990.

543 Martin, J. H., Knauer, G. A., Karl, D. M. and Broenkow, W. W.: Vertex - Carbon Cycling in  
544 the Northeast Pacific, *Deep. Res. Part A*, 34(2), 267–285 [online] Available from: <Go to  
545 ISI>://A1987G837500008, 1987b.

546 Mayor, D. J., Sanders, R., Giering, S. L. C. and Anderson, T. R.: Microbial gardening in the  
547 ocean's twilight zone, *Bioessays*, 36(12), 1132–7, doi:10.1002/bies.201400100, 2014.

548 Le Moigne, F. A. C., Henson, S. A., Cavan, E., Georges, C., Pabortsava, K., Achterberg, E.  
549 P., Ceballos-Romero, E., Zubkov, M. and Sanders, R. J.: What causes the inverse relationship  
550 between primary production and export efficiency in the Southern Ocean?, *Geophys. Res.  
551 Lett.*, doi:10.1002/2016GL068480, 2016.

552 Le Moigne, F., Sanders, R., Villa-Alfageme, M., Martin, A. P., Pabortsava, K., Planquette,  
553 H., Morris, P. and Thomalla, S.: On the proportion of ballast versus non-ballast associated  
554 carbon export in the surface ocean, *Geophys. Res. Lett.*, 39(15), doi:10.1029/2012GL052980,  
555 2012.

556 Van Mooy, B. A. S., Keil, R. G. and Devol, A. H.: Impact of suboxia on sinking particulate  
557 organic carbon : Enhanced carbon flux and preferential degradation of amino acids via  
558 denitrification, *Geochim. Cosmochim. Acta*, 66(3), 457–465, 2002.

559 Parekh, P., Dutkiewicz, S., Follows, M. J. and Ito, T.: Atmospheric carbon dioxide in a less  
560 dusty world, *Geophys. Res. Lett.*, 33, doi:doi:10.1029/2005GL025098, 2006.

561 Park, J., Oh, I.-S., Kim, H.-C. and Yoo, S.: Variability of SeaWiFs chlorophyll-a in the  
562 southwest Atlantic sector of the Southern Ocean: Strong topographic effects and weak  
563 seasonality, *Deep Sea Res. Part I Oceanogr. Res. Pap.*, 57(4), 604–620,  
564 doi:10.1016/j.dsr.2010.01.004, 2010.

565 Paulmier, A. and Ruiz-Pino, D.: Oxygen minimum zones (OMZs) in the modern ocean, *Prog.  
566 Oceanogr.*, 80(3-4), 113–128, doi:10.1016/j.pocean.2008.08.001, 2009.

567 Pollard, R. T., Salter, I., Sanders, R. J., Lucas, M. I., Moore, C. M., Mills, R. A., Statham, P.  
568 J., Allen, J. T., Baker, A. R., Bakker, D. C. E., Charette, M. A., Fielding, S., Fones, G. R.,  
569 French, M., Hickman, A. E., Holland, R. J., Hughes, J. A., Jickells, T. D., Lampitt, R. S.,  
570 Morris, P. J., Nedelec, F. H., Nielsdottir, M., Planquette, H., Popova, E. E., Poulton, A. J.,



571 Read, J. F., Seeyave, S., Smith, T., Stinchcombe, M., Taylor, S., Thomalla, S., Venables, H.  
572 J., Williamson, R. and Zubkov, M. V: Southern Ocean deep-water carbon export enhanced by  
573 natural iron fertilization, *Nature*, 457(7229), 577–U81, doi:Doi 10.1038/Nature07716, 2009.

574 Puigcorbé, V., Benitez-Nelson, C. R., Masqué, P., Verdeny, E., White, A. E., Popp, B. N.,  
575 Prahl, F. G. and Lam, P. J.: Small phytoplankton drive high summertime carbon and nutrient  
576 export in the Gulf of California and Eastern Tropical North Pacific, *Global Biogeochem.*  
577 *Cycles*, 29(8), 1309–1332, doi:10.1002/2015GB005134, 2015.

578 Redfield, A. C.: On the proportions of organic derivatives in sea water and their relation to  
579 the composition of plankton, University Press of Liverpool., 1934.

580 Riley, J., Sanders, R., Marsay, C., Le Moigne, F., Achterberg, E. and Poulton, A.: The  
581 relative contribution of fast and slow sinking particles to ocean carbon export, *Global*  
582 *Biogeochem. Cycles*, 26, doi:doi:10.1029/2011GB004085, 2012.

583 Romero-Ibarra, N. and Silverberg, N.: The contribution of various types of settling particles  
584 to the flux of organic carbon in the Gulf of St. Lawrence, *Cont. Shelf Res.*, 31(16), 1761–  
585 1776, doi:10.1016/j.csr.2011.08.006, 2011.

586 Salter, I., Lampitt, R. S., Sanders, R., Poulton, A., Kemp, A. E. S., Boorman, B., Saw, K. and  
587 Pearce, R.: Estimating carbon, silica and diatom export from a naturally fertilised  
588 phytoplankton bloom in the Southern Ocean using PELAGRA: A novel drifting sediment  
589 trap, *Deep. Res. Part II-Topical Stud. Oceanogr.*, 54(18-20), 2233–2259,  
590 doi:10.1016/j.dsr2.2007.06.008, 2007.

591 Sanders, R., Henson, S. A., Koski, M., De La Rocha, C. L., Painter, S. C., Poulton, A. J.,  
592 Riley, J., Salihoglu, B., Visser, A., Yool, A., Bellerby, R. and Martin, A. P.: The Biological  
593 Carbon Pump in the North Atlantic, *Prog. Oceanogr.*, 129, 200–218,  
594 doi:10.1016/j.pocean.2014.05.005, 2014.

595 Smythe-Wright, D., Boswell, S., Kim, Y.-N. and Kemp, A.: Spatio-temporal changes in the

596 distribution of phytopigments and phytoplanktonic groups at the Porcupine Abyssal Plain  
597 (PAP) site, *Deep Sea Res. Part II Top. Stud. Oceanogr.*, 57(15), 1324–1335,  
598 doi:10.1016/j.dsr2.2010.01.009, 2010.

599 Takahashi, T., Sutherland, S., Sweeney, C., Poisson, A., Metzl, N., Tilbrook, B., Bates, N.,  
600 Wanninkhof, R., Feely, R., Sabine, C., Olafsson, J. and Nojiri, Y.: Global sea–air CO<sub>2</sub> flux  
601 based on climatological surface ocean pCO<sub>2</sub>, and seasonal biological and temperature effects,  
602 *Deep Sea Res. Part II Top. Stud. Oceanogr.*, 49(9-10), 1601–1622, doi:10.1016/S0967-  
603 0645(02)00003-6, 2002.

604 Tarling, G. A., Shreeve, R., Ward, P. and Hirst, A.: Life-cycle phenotypic composition and  
605 mortality of *Calanoides actus* in the Scotia Sea; a modeling approach, *Mar. Ecol. Prog. Ser.*,  
606 272, 165–181, 2004.

607 Williams, R. L., Wakeham, S., McKinney, R. and Wishner, K. F.: Trophic ecology and  
608 vertical patterns of carbon and nitrogen stable isotopes in zooplankton from oxygen  
609 minimum zone regions, *Deep. Res. Part I Oceanogr. Res. Pap.*, 90(1), 36–47,  
610 doi:10.1016/j.dsr.2014.04.008, 2014.

611 Wilson, S., Steinberg, D. and Buesseler, K.: Changes in fecal pellet characteristics with depth  
612 as indicators of zooplankton repackaging of particles in the mesopelagic zone of the  
613 subtropical and subarctic North Pacific Ocean, *Deep. Res. Part II-Topical Stud. Oceanogr.*,  
614 55(14-15), 1636–1647, doi:10.1016/j.dsr2.2008.04.019, 2008.

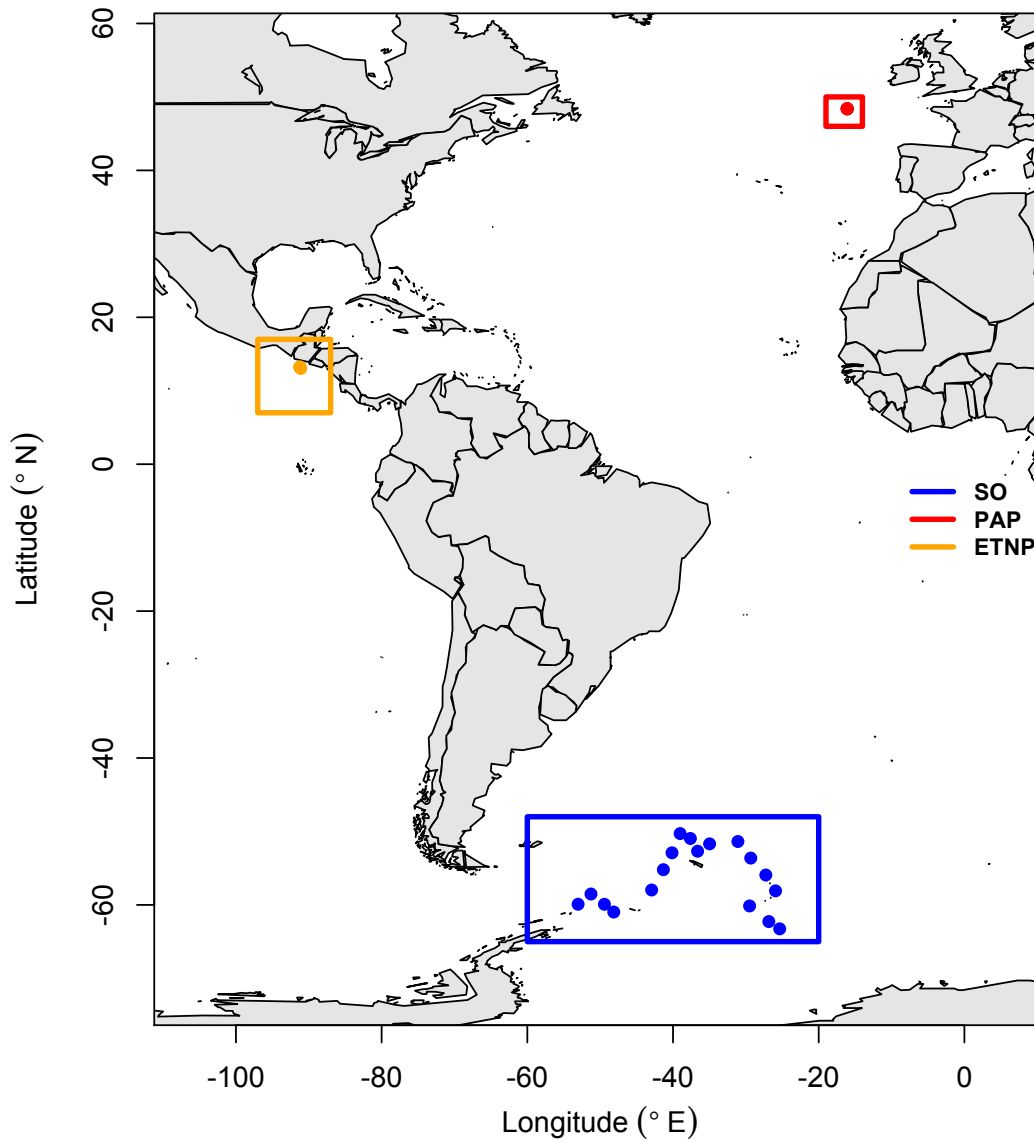
615 Wilson, S., Ruhl, H. and Smith, K.: Zooplankton fecal pellet flux in the abyssal northeast  
616 Pacific : A 15 year time-series study, *Limnol. Oceanogr.*, 58(3), 881–892,  
617 doi:10.4319/lo.2013.58.3.0881, 2013.

618 Wishner, K. F., Outram, D. M., Seibel, B. A., Daly, K. L. and Williams, R. L.: Zooplankton  
619 in the eastern tropical north Pacific: Boundary effects of oxygen minimum zone expansion,  
620 *Deep Sea Res. Part I Oceanogr. Res. Pap.*, 79, 122–140, doi:10.1016/j.dsr.2013.05.012, 2013.

621 Yool, A., Popova, E. E. and Anderson, T. R.: MEDUSA-2.0: an intermediate complexity  
622 biogeochemical model of the marine carbon cycle for climate change and ocean acidification  
623 studies, *Geosci. Model Dev.*, 6(5), 1767–1811, doi:10.5194/gmd-6-1767-2013, 2013.

624

625



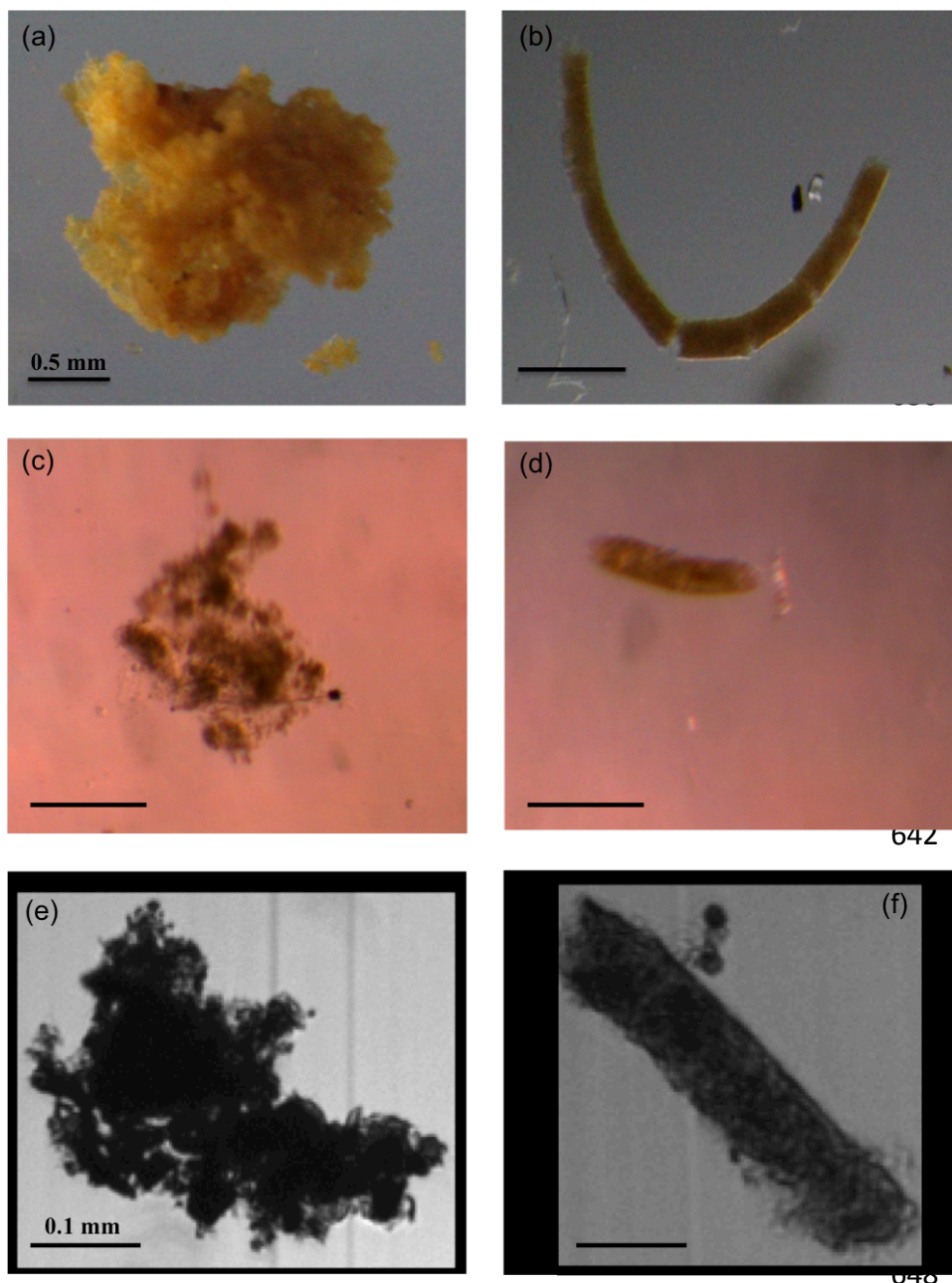
626

627 **Fig. 1.** Map showing study areas. Blue rectangle is location of sites in the Southern Ocean,

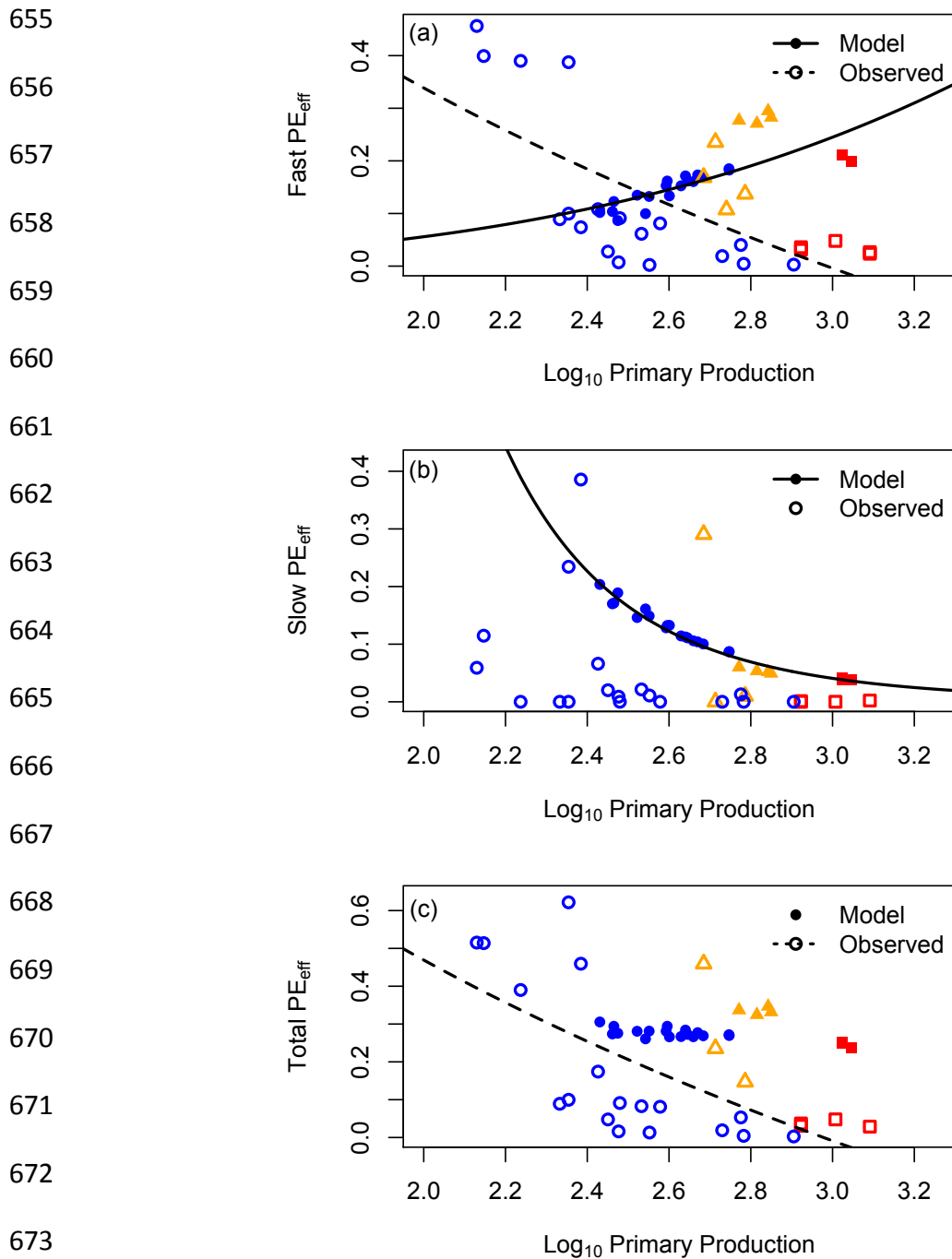
628 red is the North Atlantic Porcupine Abyssal Plain and orange the equatorial north Pacific

629 oxygen minimum zone.

630

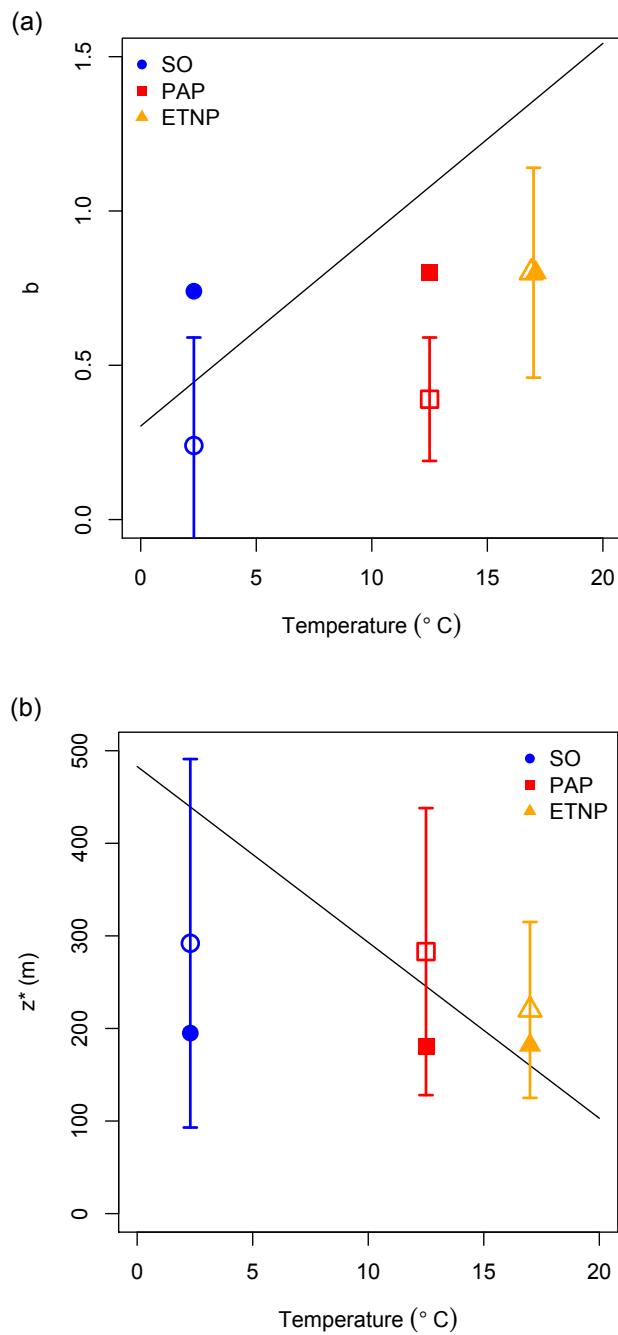


649 **Fig. 2.** Particle images from the 3 different regions; Southern Ocean (a & b), PAP site (c & d)  
 650 and the ETNP (e & f). a, c & e are phytodetrital aggregates and b, d & f are faecal pellets. b is  
 651 a chain of krill pellets from the SO and d & f are copepod pellets. Scale bars are 0.5 mm for  
 652 the SO and PAP images (a-d) and 0.1 mm for the ETNP (e & f). A stereomicroscope was  
 653 used in the SO, a compound microscope at PAP and a FlowCAM in the ETNP, giving rise to  
 654 the different background colours and shades.

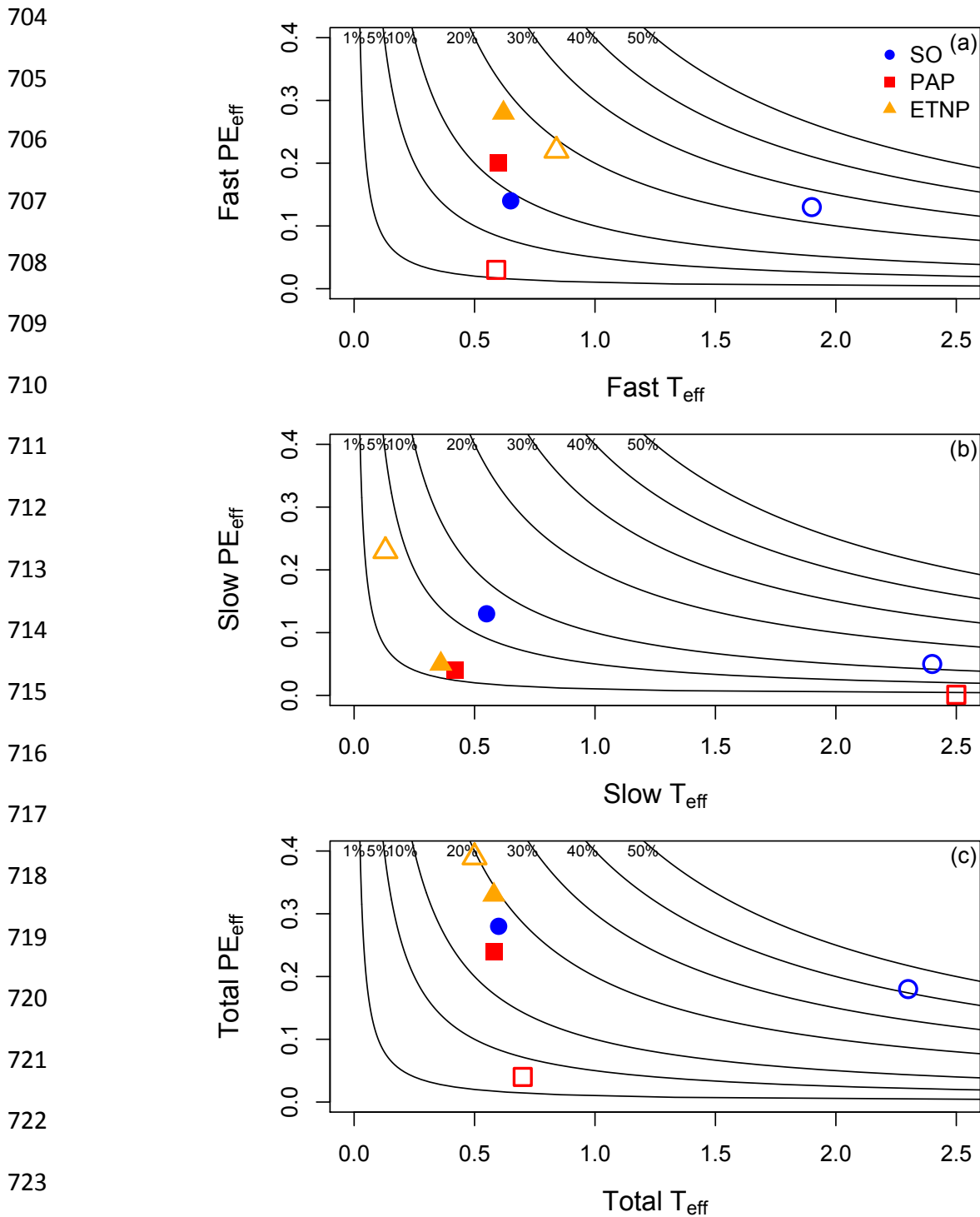


674 **Fig. 3.** Primary production against particle export efficiency ( $\text{PE}_{\text{eff}}$ ) for (a) fast sinking, (b)  
 675 slow sinking and (c) total sinking particles. Blue circles are Southern Ocean, red squares PAP  
 676 and orange triangles equatorial Pacific. Filled circles and solid black lines show model output  
 677 and open circles and dashed lines are observations. All fitted lines are statistically significant  
 678 to at least the 95 % level (see text for details).

679  
680  
681  
682  
683  
684  
685  
686  
687  
688  
689  
690  
691  
692  
693  
694  
695  
696  
697



698 **Fig. 4.** Total sinking POC attenuation coefficients (a)  $b$  and (b)  $z^*$  with temperature. Blue  
699 circles are Southern Ocean, red squares PAP and orange triangles equatorial Pacific. Filled  
700 points show model output and open points are observations. Solid line is Marsay et al. (2015)  
701 regression. Error bars are standard error of the mean and only plotted on the observations as  
702 the error is too small in the model. See Table S2 for attenuation coefficients of fast and slow  
703 sinking particles.



724 **Fig. 5.** Efficiency of the biological carbon pump for (a) fast, (b) slow and (c) total sinking  
 725 particles. Particle export efficiency (PE<sub>eff</sub>) is plotted against transfer efficiency (T<sub>eff</sub>).  
 726 Contours represent BCPEff (proportion of primary production reaching depths of 150-300 m).  
 727 Blue circles are Southern Ocean, red squares PAP and orange triangles equatorial Pacific.  
 728 Filled points show model output and open points are observations.